ELSEVIER

Catalysis Today 71 (2001) 153–159

CATALYSIS TODAY

www.elsevier.com/locate/cattod

Hydrothermal synthesis of novel crystalline Mo–V–M–O (M = Al, Ga, Fe) mixed oxide in the presence of triethylammonium chloride and their catalytic performance for selective ethane oxidation

Kenzo Oshihara [a,*], Yasuhiro Nakamura [a], Mayumi Sakuma [a], Wataru Ueda [b]

[a] *Department of Materials Science and Engineering, Science University of Tokyo in Yamaguchi, Daigaku-dori 1-1-1, Onoda, Yamaguchi 756-0884, Japan*

[b] *Catalysis Research Center, Hokkaido University, Kita 11-jo, Nishi 10, Sapporo, Hokkaido 060-0811, Japan*

Abstract

Novel crystalline Mo–V–M–O (M = Al, Ga, Fe) mixed oxides were prepared by hydrothermal synthesis with Anderson-type heteropolymolybdate and vanadyl sulfate at 175 °C in the presence of $(C_2H_5)_3NHCl$. The obtained $Mo_6V_2Al_1O_x$ mixed oxide was rod-shaped crystal and the X-ray diffraction (Cu Kα) peaks at $2\theta = 4.7$ and 8.2° were observed, which suggest a formation of a super structure in the cross-section of the rod-shaped crystal. The synthesized Mo–V–M–O (M = Al, Ga, Fe) mixed oxides were assumed the same structure of hexagonal unit cell of the space group *P*6. The mixed oxides after calcination in N_2 flow at 500 °C were used for ethane selective oxidation. The catalysts prepared in the presence of $(C_2H_5)_3NHCl$ showed higher ethane conversion and selectivity to acetic acid than those prepared in the absence of $(C_2H_5)_3NHCl$.

Keywords: Molybdenum–vanadium mixed oxide catalyst; Triethylammonium chloride; Hydrothermal synthesis; Ethane oxidation

1. Introduction

The natural gas is one of the huge resources, which consists mainly of light alkanes. Alkanes are generally less reactive because the molecules have only saturated C–H bonds. In order to utilize the less reactive molecules, the selective oxidation of alkanes has been widely investigated [1] and many types of catalysts have been developed for this process [2]. One of the most successful catalysts is crystalline V–P–O mixed oxides for the selective oxidation of *n*-butane to maleic anhydride [3,4]. The catalyst is a hexagonal-layered crystal and the (1 0 0) plane is known to be active and selective to maleic anhydride [5,6]. Mo–V–Te–Nb–O mixed oxide is also a successful catalyst for the ammoxidation of propane to acrylonitrile [7] and for the oxidation to acrylic acid [8]. The catalyst showed over 80% propane conversion and over 60% selectivity to acrylonitrile or acrylic acid. It was emphasized that a specific crystal structure is effective for the propane ammoxidation.

In the both cases, structural arrangement of active sites is considered to be quite important to achieve selective oxidation. Selective oxidation pathway from alkanes to desired oxygenates may consist of many reaction steps, for example, dehydrogenation, oxygen insertion, hydration and so on. These reactions should occur quickly and sequentially to avoid undesired oxidation to CO_x because intermediate products are generally more reactive than alkanes. In order to

* Corresponding author. Tel.: +81-836-88-4559; fax: +81-836-88-4559.
E-mail address: oshihara@ed.yama.sut.ac.jp (K. Oshihara).

0920-5861/01/$ – see front matter
PII: S0920-5861(01)00451-5

achieve the quick sequential reaction, catalytically active elements for the reactions should be placed geometrically near to each other. If we construct surface matrix having ordered active sites on catalysts, high activity and selectivity can be expected. In this sense, well-crystallized mixed oxides are the candidates for active and selective catalysts for alkane oxidation. In this paper, we focused on hydrothermally synthesized Mo–V–M–O (M = Al, Ga, Fe) mixed oxides, which are found active for the ethane oxidation [9]. For the purpose of constructing surface matrix having arranged active sites, we tried the hydrothermal synthesis of the Mo–V–M–O (M = Al, Ga, Fe) mixed oxides in the presence of $(C_2H_5)_3NHCl$. On the basis of the observed effects of $(C_2H_5)_3NHCl$ on crystal growth, the role of $(C_2H_5)_3NHCl$ is discussed. The mixed oxides were used for ethane oxidation after calcination in N_2 and the catalytic activities were compared with those of the mixed oxides synthesized in the absence of $(C_2H_5)_3NHCl$. We also discuss about the implication between the well-crystallized active face and the activity and product distribution of ethane oxidation.

2. Experimental

2.1. Catalyst preparation

All the catalysts were prepared by the hydrothermal reaction between Anderson-type heteropolymolybdates ($(NH_4)_3H_6M^{III}Mo_6O_{24}\cdot 7H_2O$) and vanadyl sulfate. The Anderson-type heteropolymolybdates were prepared by the reaction between $(NH_4)_6Mo_7O_{24}\cdot 4H_2O$ and metal sulfates (or alum), such as, $Al_2(SO_4)_3\cdot nH_2O$, $Ga_2(SO_4)\cdot 4H_2O$ or $FeNH_4(SO_4)_2\cdot 12H_2O$ [10]. Five millimoles of the corresponding Anderson-type heteropolymolybdate was dissolved or suspended into 20 ml of distilled water and heated to 80 °C (in the case of the preparation of M = Al, Ga) or 50 °C (M = Fe). The liquid was changed into slurry with color of green (M = Al) or dark purple (M = Ga, Fe) after the $VOSO_4$ aqueous solution was added. The loading amount of $VOSO_4$ was controlled to achieve the atomic ratio of Mo:V:Al = 6:1:1, Mo:V:Ga = 6:2:1 or Mo:V:Fe = 6:3:1, respectively. The aqueous solution of $(C_2H_5)_3NHCl$ was finally added into the synthetic liquid at the concentrations from 0.00 to 0.24 mol l^{-1}. The slurry was moved to an autoclave with PTFE inner tube and was kept under hydrothermal condition at 175 °C for 24 h. After hydrothermal synthesis, the autoclave was cooled to room temperature by flowing water. Inside the tube, dark purple solids were produced on the wall and the bottom. The solid was filtered, washed three times with 20 ml of distilled water and finally dried in air at 80 °C for 6 h.

2.2. Characterization of the mixed oxides

The mixed oxides were characterized by XRD (Rigaku RINT Ultima$^+$ equipped with Cu Kα) after the hydrothermal synthesis and calcination. They are also analyzed by FTIR spectra on Perkin-Elmer Paragon 1000 after the hydrothermal synthesis. The SEM images of the mixed oxides were also taken by JEOL JSM-T100 after drying. The BET surface area were measured by nitrogen adsorption at 77 K with 30% N_2 balanced He flow on Micromeritics Flowsorb 230 after ethane oxidation. A residue of chlorine in the mixed oxides was checked by XPS (Shimadzu/Kratos AXIS-HS).

2.3. Ethane oxidation

Ethane oxidation was performed on a fixed-bed flow system at the reaction temperature of 340 °C. One gram of the mixed oxide was used after the calcination in 50 ml min^{-1} N_2 flow at 500 °C. The mixed oxide was purged with 50 ml min^{-1} N_2 flow and heated to 300 °C. Then, a feed gas was introduced, which contained C_2H_6, O_2, N_2 and water vapor at the flow rate of 15, 5, 20 and 10 ml min^{-1}, respectively. Both the feed gas and the effluent gas were analyzed by gas chromatography.

3. Results and discussion

3.1. Characterization of Mo–V–M–O mixed oxides (M = Al, Ga, Fe)

XRD patterns of the Mo–V–M–O mixed oxides (M = Al, Ga, Fe) after drying are displayed in Fig. 1. When the hydrothermal syntheses were carried out in the presence of $(C_2H_5)_3NHCl$, the well-crystallized

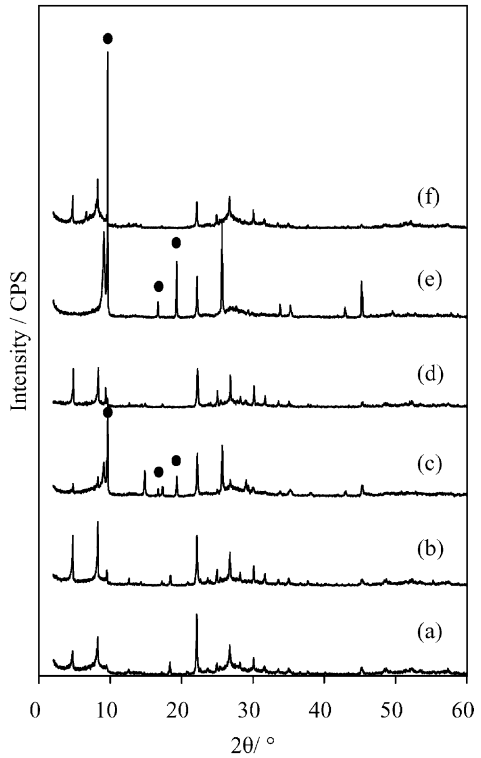

Fig. 1. XRD patterns of the hydrothermally synthesized Mo–V–M–O (M = Al, Ga, Fe) mixed oxides in the absence or presence of $(C_2H_5)_3NHCl$: (a) $Mo_6V_1Al_1O_x$; (b) $Mo_6V_1Al_1O_x$ in the presence of 0.16 mol l^{-1} $(C_2H_5)_3NHCl$; (c) $Mo_6V_2Ga_1O_x$; (d) $Mo_6V_2Ga_1O_x$ in the presence of 0.16 mol l^{-1} $(C_2H_5)_3NHCl$; (e) $Mo_6V_3Fe_1O_x$ and (f) $Mo_6V_3Fe_1O_x$ in the presence of 0.52 mol l^{-1} $(C_2H_5)_3NHCl$.

Mo–V–M–O mixed oxides (M = Al, Ga, Fe) were obtained for the first time (Fig. 1b, d and f). All the mixed oxides synthesized in the presence of $(C_2H_5)_3NHCl$ gave the same diffraction patterns assigned to the hexagonal unit cell of the space group *P*6 with the lattice parameters, $a_0 = 21.38$ Å and $c_0 = 4.006$ Å for $Mo_6V_1Al_1O_x$, $a_1 = 21.43$ Å and $c_1 = 4.010$ Å for $Mo_6V_2Ga_1O_x$ and $a_2 = 21.44$ Å and $c_2 = 4.012$ Å for $Mo_6V_3Fe_1O_x$, respectively. This clearly indicates that the obtained Mo–V–M–O (M = Al, Ga, Fe) mixed oxides are the same structural materials having the super structure.

On the other hand, when the $Mo_6V_2Ga_1O_x$ and $Mo_6V_3Fe_1O_x$ mixed oxides were synthesized in the absence of $(C_2H_5)_3NHCl$, the two peaks at $2\theta = 22.1$ and 45.2° ascribed to the Mo–V–O-based mixed oxides [11] were mainly observed, but no peaks at the low angle region were observed, indicating the absence of the super structure. Additionally, the peaks ascribed to the NH_3MoO_3 were observed at $2\theta = 9.6$, 19.4 and 25.8° (Fig. 1c and e). In the case when the $Mo_6V_1Al_1O_x$ mixed oxide was synthesized in the absence of $(C_2H_5)_3NHCl$, though the peaks were observed at the low angle region, the peak intensities at $2\theta = 4.7$ and 8.2° were very weak. It is clear that $(C_2H_5)_3NHCl$ promotes the crystallization to the particular directions of the mixed oxide crystal.

The effect of the concentration of $(C_2H_5)_3NHCl$ on the crystallization of the $Mo_6V_1Al_1O_x$ mixed oxides in the hydrothermal synthesis was examined and the results are displayed in Fig. 2. It was clearly shown that the intensities of the peaks at $2\theta = 4.7$

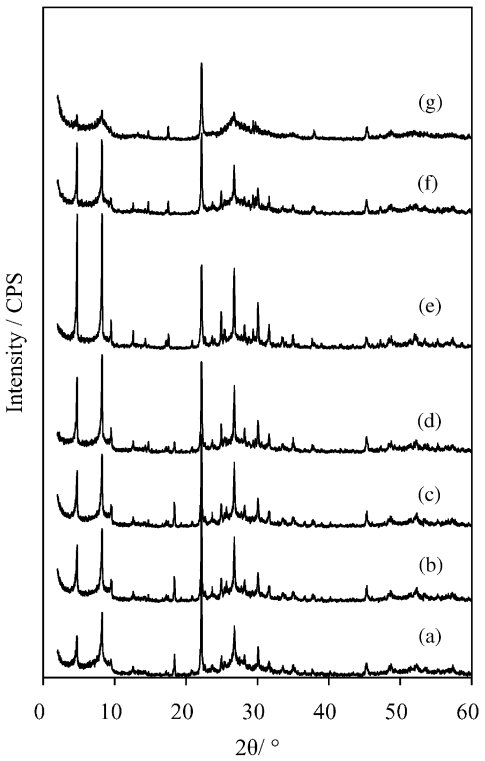

Fig. 2. Effect of the $(C_2H_5)_3NHCl$ concentration on the XRD patterns of the $Mo_6V_1Al_1O_x$ mixed oxide: (a) in the absence of $(C_2H_5)_3NHCl$; (b) in the presence of $(C_2H_5)_3NHCl$ at the concentration of 0.04 mol l^{-1}; (c) 0.08 mol l^{-1}; (d) 0.12 mol l^{-1}; (e) 0.16 mol l^{-1}; (f) 0.20 mol l^{-1} and (g) 0.24 mol l^{-1}.

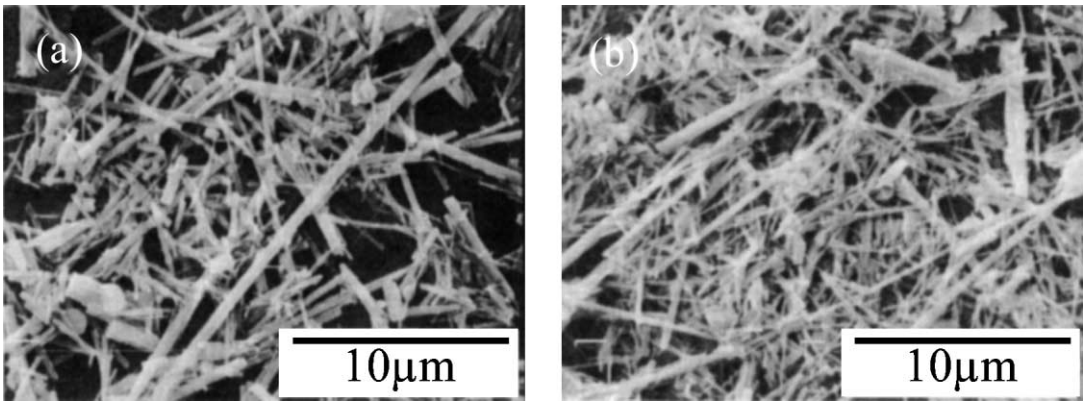

Fig. 3. The SEM images of the hydrothermally synthesized $Mo_6V_1Al_1O_x$ mixed oxides: (a) $Mo_6V_1Al_1O_x$ synthesized in the presence of 0.16 mol l^{-1} $(C_2H_5)_3NHCl$ and (b) $Mo_6V_1Al_1O_x$ synthesized in the absence of $(C_2H_5)_3NHCl$.

and 8.2° were increased with the increase of the $(C_2H_5)_3NHCl$ concentration. But when the concentration was increased beyond 0.16 mol l^{-1}, the intensities of the peaks were decreased. Fig. 3 shows the SEM images of the $Mo_6V_1Al_1O_x$ mixed oxides hydrothermally synthesized in the presence or the absence of $(C_2H_5)_3NHCl$. Rod-shaped crystals were observed for the mixed oxides prepared both in the presence and in the absence of $(C_2H_5)_3NHCl$, but the thickness of the crystal was apparently higher when the mixed oxide was synthesized in the presence of $(C_2H_5)_3NHCl$. Since, the XRD peaks at $2\theta = 4.7$ and 8.2° may correspond to the diffraction from the (1 0 0) and (1 1 0) planes, which is parallel to the cross-section of the rod-shaped crystal, the increase of their peak intensities means the increase of crystallinity of the cross-section. All these results clearly shows that $(C_2H_5)_3NHCl$ promotes the crystallization of the cross-section of the rod-shaped crystal.

The mixed oxides were analyzed by FTIR after the hydrothermal synthesis. The spectra are shown in Fig. 4. Since, we could not observe the peaks ascribed to $(C_2H_5)_3NHCl$, the remaining of $(C_2H_5)_3NHCl$ in the Mo–V–M–O mixed oxide can be excluded. The peak at 711 cm^{-1} was increased when the mixed oxide was synthesized in the presence of $(C_2H_5)_3NHCl$. This may be due to the increase of Mo (or V)–O–Mo bond, indicating that the crystallinity of the mixed oxide was increased. The peak at 1400 cm^{-1} assigned to N–H stretching of ammonium cation was observed for all the mixed oxides. The presence of ammonium

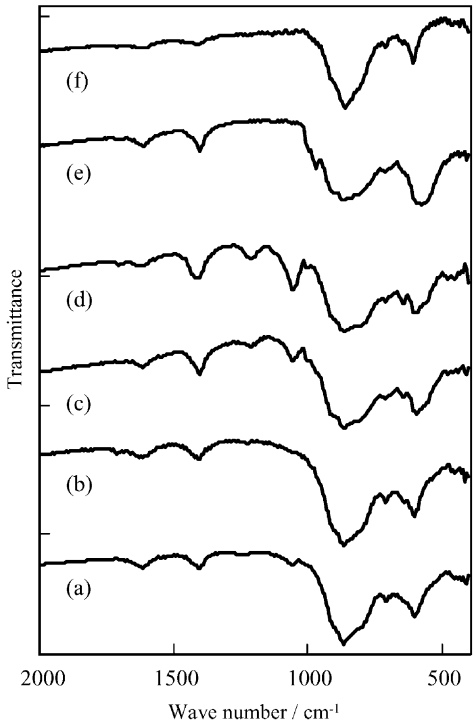

Fig. 4. The FTIR spectra of the hydrothermally synthesized Mo–V–M–O (M = Al, Ga, Fe) mixed oxides in the absence or presence of $(C_2H_5)_3NHCl$: (a) $Mo_6V_1Al_1O_x$; (b) $Mo_6V_1Al_1O_x$ in the presence of 0.16 mol l^{-1} $(C_2H_5)_3NHCl$; (c) $Mo_6V_2Ga_1O_x$; (d) $Mo_6V_2Ga_1O_x$ in the presence of 0.16 mol l^{-1} $(C_2H_5)_3NHCl$; (e) $Mo_6V_3Fe_1O_x$ and (f) $Mo_6V_3Fe_1O_x$ in the presence of 0.52 mol l^{-1} $(C_2H_5)_3NHCl$.

cation indicates that the mixed oxides can have an acidic property. In the case of $Mo_6V_2Ga_1O_x$ and $Mo_6V_3Fe_1O_x$ mixed oxide synthesized in the absence of $(C_2H_5)_3NHCl$, the peaks at 970 and 1004 cm^{-1} were observed. These peaks can be assigned to Mo=O bond of the NH_3MoO_3 because of which, it was detected by XRD analysis.

3.2. Hydrothermal synthesis in the presence of $(C_2H_5)_3NHCl$

In order to explain why the crystalline Mo–V–M–O (M = Al, Ga, Fe) was obtained when it was synthesized in the presence of $(C_2H_5)_3NHCl$, we consider the reactions during the hydrothermal synthesis. Anderson-type heteropolymolybdate anion is a flat-shaped polyoxometalate, which consists of octahedra of the heteroatom surrounded by six octahedras of molybdenum with edge-sharing [12]. Since, the rod-shaped crystal has a layer structure with *d*-spacing of 4 Å corresponding the sized of MoO_6 octahedra, the flat-shaped Anderson-type heteropolymolybdate may be placed aslope in the rod-shaped crystal. During the hydrothermal synthesis, the vanadyl cation may coordinate on the flat face of the heteropolymolybdate anion at MoO_6 octahedra and another vanadyl cation may also coordinate on the opposite side at other MoO_6 octahedra placed across the heteroatom. Another heteropolymolybdate coordinates on the vanadyl cation that already coordinated to one polymolybdate. By repeating this process, Anderson-vanadyl zigzag chain can be formed. In this reaction, the vanadyl cation can be regarded as a 'linker' of Anderson-type heteropolymolybdate as a 'building unit' [13,14]. Finally these zigzag chains are gathered to form the rod-shaped crystal through the condensation reaction between Mo (or V) octahedra. If the vanadyl cation coordinates on heteropolymolybdate at more than three point, the 'Anderson-vanadyl' chain becomes branched. Since, the branched chain snags the gathering of the chains, the crystallinity of the cross-section of the rod-shaped crystal becomes low. Therefore, we can estimate that the crystallinity of the cross-section becomes lower when the concentration of $VOSO_4$ is increased. In fact, the peaks at $2\theta = 4.7$ and 8.2° corresponding to the crystallization of the cross-section was decreased with the increase of $VOSO_4$ concentration (Fig. 5).

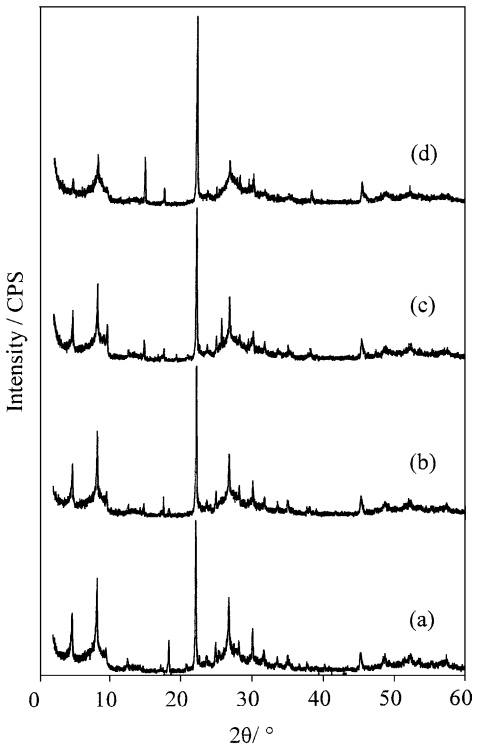

Fig. 5. XRD patterns of the hydrothermally synthesized $Mo_6V_xAl_1O_y$ mixed oxides (y = 1–3): (a) $Mo_6V_1Al_1O_y$; (b) $Mo_6V_{1.5}Al_1O_y$; (c) $Mo_6V_2Al_1O_y$ and (d) $Mo_6V_3Al_1O_y$.

If the mixed oxide is synthesized in the presence of $(C_2H_5)_3NHCl$, the $(C_2H_5)_3NH^+$ cation coordinates to the hydrophobic Mo=O bond of the heteropolymolybdate at the ethyl group. Since, bulky ligand like $(C_2H_5)_3NH^+$ prevents multi-coordination of the vanadyl cation to heteropolymolybdate, the less branched chains are formed. The less branched chains are gathered by the coordination of another ethyl group of the $(C_2H_5)_3NH^+$ to the Mo=O bond of another heteropolymolybdate chain and finally, the octahedra are condensed through the hydrolysis to form the rod-shaped crystal having the highly crystallized cross-section. However, $(C_2H_5)_3NH^+$ does not remain in the mixed oxide crystals because the XRD peak positions were not changed and the peaks ascribed to $(C_2H_5)_3NHCl$ were not observed in the FTIR spectra (Fig. 4). We speculate that the coordinated $(C_2H_5)_3NH^+$ was hydrolyzed during the chain-gathering process to form C_2H_5OH because

Table 1
The results of ethane oxidation over the Mo–V–M–O (M = Al, Fe, Ga) mixed oxide catalysts[a]

Catalysts	$(C_2H_5)_3NHCl$ ($mol\,l^{-1}$)	Conversion (%)		Selectivity (%)			
		C_2H_6	O_2	CH_3COOH	C_2H_4	CO	CO_2
$Mo_6V_1Al_1O_x$	0.00	2.4	6.1	5.3	78.4	11.1	5.2
	0.16	3.9	10.0	10.2	73.1	11.4	5.3
$Mo_6V_3Fe_1O_x$	0.00	1.8	5.7	6.0	68.2	18.0	7.8
	0.52	2.4	8.2	9.5	62.8	14.6	13.1
$Mo_6V_2Ga_1O_x$	0.00	5.6	19.6	2.8	72.1	16.1	9.1
	0.16	12.6	29.5	4.2	84.5	8.1	3.3

[a] Reaction temperature 340 °C; catalyst weight 1.0 g; C_2H_6:O_2:N_2:H_2O(vapor) = 15:5:20:10 ($ml\,min^{-1}$).

which C_2H_5OH was detected after the hydrothermal synthesis.

When the concentration of $(C_2H_5)_3NH^+$ is too high, $(C_2H_5)_3NH^+$ occupies all the opened Mo=O sites, therefore, the coordinated $(C_2H_5)_3NHCl^+$ itself snags the gathering and the high concentration of $(C_2H_5)_3NHCl$ results in the formation of the rod-shaped crystal with the ill-crystallized cross-section. Nevertheless, in the case of the $Mo_6V_3Fe_1O_x$ mixed oxide, the suitable concentration was extremely high, 0.52 $mol\,l^{-1}$ compared with 0.16 $mol\,l^{-1}$ for the $Mo_6V_1Al_1O_x$ or $Mo_6V_2Ga_1O_x$ mixed oxide. Although, the reason is not clear at present, this may be explained by the reaction between $(C_2H_5)_3NHCl$ and dissolved oxygen. Since, the iron atom of $(NH_4)_3H_6FeMo_6O_{24}$ has two oxidation states, $(NH_4)_3H_6FeMo_6O_{24}$ may catalyze the oxidation of $(C_2H_5)_3NHCl$. A considerable part of $(C_2H_5)_3NHCl$ is consumed by the oxidation, only the remaining $(C_2H_5)_3NH^+$ can work as the ligand to gather the heteropolymolybdate chain to promote the crystallization of the rod-shaped crystal. Therefore, the suitable concentration became as high as 0.52 $mol\,l^{-1}$ in the case of the $Mo_6V_3Fe_1O_x$ mixed oxide.

3.3. Catalytic activity for ethane oxidation

The Mo–V–M–O (M = Al, Ga, Fe) mixed oxide was used as a precursor of the catalysts for the ethane oxidation. The mixed oxides were calcinated in N_2 flow at 500 °C for 2 h. In the case of $Mo_6V_1Al_1O_x$ mixed oxide, since the MoO_2 peaks appeared at 2θ = 26.0, 37.0 and 53.5° with considerable decreasing of XRD peaks at 2θ = 4.7 and 8.2° after the calcination. Obviously, the mixed oxides were partly decomposed. Nevertheless, the catalysts synthesized from the well-crystallized mixed oxide precursor were found more effective for the ethane oxidation as shown in Table 1. All the Mo–V–M–O (M = Al, Ga, Fe) mixed oxides synthesized in the presence of $(C_2H_5)_3NHCl$ gave higher ethane conversion with higher selectivity to acetic acid. The contribution of chlorine produced from $(C_2H_5)_3NHCl$ should be considered because it is known that chlorine sometimes facilitates some selective oxidation [15]. But it was denied because the Cl 2p peak was not observed in XPS of the $Mo_6V_1Al_1O_x$ catalyst synthesized with 0.16 $mol\,l^{-1}$ $(C_2H_5)_3NHCl$ that gave the highest acetic acid selectivity.

When the concentration of $(C_2H_5)_3NHCl$ was increased, the ethane conversion and the selectivity to acetic acid was increased as shown in Table 2. The yield of acetic acid was increased with the increasing of $(C_2H_5)_3NHCl$ concentration, but it was decreased when the concentration was increased beyond 0.16 $mol\,l^{-1}$. Although, the surface area was increased monotonously with the $(C_2H_5)_3NHCl$ concentration, the increase of acetic acid yield seemed not due to the increase of the surface area because the mixed oxide synthesized in the presence of 0.24 $mol\,l^{-1}$ $(C_2H_5)_3NHCl$ showed low acetic acid yield in spite of the high surface area.

Since, the yield of acetic acid was increased with the intensities of XRD peaks at 2θ = 4.7 and 8.2° before calcination, it can be suggested that the well-crystallized cross-section is active and selective for ethane oxidation to acetic acid. There was no evidence at present because the diffraction peaks were disappeared after the calcination at 500 °C. However, if the fragment of the well-crystallized cross-section

Table 2
Ethane oxidation over the $Mo_6V_1Al_1O_x$ catalysts synthesized[a]

$(C_2H_5)_3NHCl$ (mol l^{-1})	BET surface area ($m^2\,g^{-1}$)	Conversion (%)		Selectivity (%)			
		C_2H_6	O_2	CH_3COOH	C_2H_4	CO	CO_2
0.00	6.0	0.6	1.3	10.4	71.3	13.1	5.1
0.08	7.1	1.5	4.4	10.0	72.2	10.6	7.2
0.16	8.6	2.1	4.1	15.7	65.5	12.7	6.0
0.24	12.0	1.3	5.3	7.0	67.3	18.1	7.6

[a] Reaction temperature 340 °C; cata1yst weight 1.0 g; C_2H_6:O_2:N_2:H_2O(vapor) = 15:5:20:10 (ml min^{-1}). The BET surface area was measured after the ethane oxidation.

having the same arrangement of active sites remain, the selective oxidation reaction could be achieved even after the partial decomposition of the catalyst structure because the particle size is large enough compared with the structure having the arranged active elements. Therefore, it can be concluded that the arrangement of the active sites is important also in the selective oxidation of ethane to acetic acid.

4. Conclusion

The well-crystallized Mo–V–M–O mixed oxides (M = Al, Ga, Fe) were synthesized for the first time by hydrothermal method in the presence of $(C_2H_5)_3NHCl$. The presence of $(C_2H_5)_3NHCl$ was found to be effective for the synthesis of the well-crystallized cross-section of the rod-shaped crystal. It was speculated that $(C_2H_5)_3NH^+$, the bulky ligand, prevents the multi-coordination of the vanadyl 'linker' to the Anderson-type heteropolymolybdate leading to the formation of the branched Anderson-vanadyl chain. The less branched Anderson-vanadyl chains are gathered by the coordination of ethyl group of $(C_2H_5)_3NH^+$ to another Anderson-vanadyl chain to form the rod-shaped crystal. The well-crystallized mixed oxide after calcination at 500 °C gave higher ethane conversion and higher selectivity to acetic acid, suggesting the well-crystallized mixed oxide is active and selective for ethane oxidation.

References

[1] R.K. Grasselli, Catal. Today 49 (1999) 141.
[2] F. Cavani, F. Trifiro, Catal. Today 51 (1999) 561.
[3] G. Centi, Catal. Today 16 (1993) 5.
[4] G.J. Hutching, Catal. Today 16 (1993) 16.
[5] V.A. Zazhigalov, J. Haber, J. Stoch, A.I. Kharlamov, L.B. Bogutskya, I.V. Bacherikova, A. Kowal, Stud. Surf. Sci. Catal. 110 (1997) 337.
[6] H.S. Horowitz, C.M. Blackstone, A.W. Sleight, G. Teufer, Appl. Catal. 38 (1988) 193.
[7] H. Watanabe, Y. Koyasu, Appl. Catal. A 194/195 (2000) 479.
[8] Mitsubishi Chemicals, JP 10-36311 (1993).
[9] W. Ueda, N.F. Chen, K. Oshihara, Kinetic Catal. 40 (1999) 401.
[10] K. Nomiya, T. Takahashi, T. Shirai, M. Miwa, Polyhedron 6 (1987).
[11] E.M. Thornsteinson, T.P. Wilson, F.G. Young, P.H. Kasai, J. Catal. 52 (1978) 116.
[12] M.T. Pope, Heteropoly and Isopoly Oxometalates, Springer, New York, 1983, p. 21.
[13] L. Cronin, P. Kogerler, A. Muller, J. Solid State Chem. 152 (2000) 57.
[14] G. Ferey, J. Solid State Chem. 152 (2000) 37.
[15] W. Ueda, S.W. Lin, I. Tohmoto, Catal. Lett. 44 (1997) 137.